APL Materials

Bandgap calculations and trends of organometal halide perovskites

Cite as: APL Mater. **2**, 081514 (2014); https://doi.org/10.1063/1.4893495
Submitted: 30 April 2014 . Accepted: 06 August 2014 . Published Online: 26 August 2014

Ivano E. Castelli, Juan María García-Lastra, Kristian S. Thygesen, and Karsten W. Jacobsen

Bandgap calculations and trends of organometal halide perovskites

Ivano E. Castelli,[1,a] Juan María García-Lastra,[1,2] Kristian S. Thygesen,[1] and Karsten W. Jacobsen[1]
[1]*Center for Atomic-scale Materials Design (CAMD), Department of Physics, Technical University of Denmark, DK 2800 Kgs. Lyngby, Denmark*
[2]*Department of Energy Conversion and Storage, Technical University of Denmark, DK 4000 Roskilde, Denmark*

(Received 30 April 2014; accepted 6 August 2014; published online 26 August 2014)

Energy production from the Sun requires a stable efficient light absorber. Promising candidates in this respect are organometal perovskites (ABX_3), which have been intensely investigated during the last years. Here, we have performed electronic structure calculations of 240 perovskites composed of Cs, CH_3NH_3, and $HC(NH_2)_2$ as A-cation, Sn and Pb as B-ion, and a combination of Cl, Br, and I as anions. The calculated gaps span over a region from 0.5 to 5.0 eV. In addition, the trends over bandgaps have been investigated: the bandgap increases with an increase of the electronegativities of the constituent species, while it reduces with an increase of the lattice constants of the system. [http://dx.doi.org/10.1063/1.4893495]

As the adverse environmental consequences of fossil energy use are growing, the search for new efficient technologies enabling conversion of solar photons into electrical or chemical energy is becoming increasingly important. In this respect organometal halide perovskite (OMHP) based solar cells have arisen as one of the innovative photovoltaic technologies in recent times, mostly because of their direct bandgap, large light absorption coefficients due to a direct transition at the bandgap that involves Pb s-states and Pb p-states and high carrier mobility.[1,2] For instance, power conversion efficiency achieved with $CH_3NH_3PbI_3$ has now surpassed 15%, making them competitive with photovoltaic thin films.[3–8]

To improve the efficiency of solar cells based on OMHPs further it is natural to resort to computational methods that allow for fast exploration of the vast space of material composition and structures. Thanks to the enormous growth in computer power, high-throughput computational screening is rapidly becoming an essential tool for accelerated materials discovery and has recently been applied within a wide range of areas.[9–15]

In our study, we have selected the three most common symmetries for this group of perovskites (cubic, tetragonal, and two orthorhombic phases with space groups $P_{m\bar{3}m}$, $P_{4/mbm}$, P_{bnm}, and P_{nma}, respectively) with general formula unit (fu) ABX_3 where A is one of cesium (Cs^+), methylammonium (MA: $CH_3NH_3^+$), and formamidinium (FA: $HC(NH_2)_2^+$); tin (Sn^{2+}) or lead (Pb^{2+}) occupies the B-ion position, and chlorine, bromine, iodine, and their combination are used as anions (X_3^{3-}: Cl_3, Br_3, I_3, Cl_2Br, $ClBr_2$, Cl_2I, ClI_2, Br_2I, BrI_2, ClBrI). The ideal investigated structures are shown in Fig. 1. Here we focus on the calculation of the stability and bandgaps of all these possible combinations.

A total of 240 organic perovskites have been studied using the density functional theory (DFT) code GPAW.[16,17] We have investigated the performances of different functionals for evaluating the lattice constants for the set of systems including $CsSnCl_3$, $CsSnBr_3$, $CsSnI_3$, $CsPbCl_3$, $CsPbBr_3$, $CsPbI_3$, $MASnCl_3$, $MASnBr_3$, $MASnI_3$, $MAPbCl_3$, $MAPbBr_3$, $MAPbI_3$, and $FASnI_3$. The local density approximation (LDA)[18] and the generalized gradient approximation (GGA) functional from

[a]Electronic mail: ivca@fysik.dtu.dk

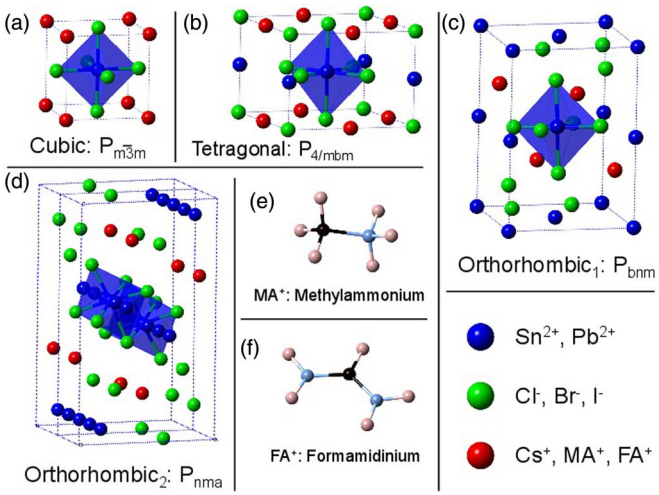

FIG. 1. Crystal structures investigated in this work: cubic (a), tetragonal (b), and orthorhombic (c and d). The tetragonal and orthorhombic phases, with 20 atoms unit cell, differ from the cubic (5 atoms unit cell) by a planar rotation and a tilting of the octahedron, respectively. The organic molecules are shown in (e) and (f).

Perdew-Becke-Ernzerhof (PBE)[19] show a Mean Absolute Error (MAE) larger than 10 pm (14.4 and 11.1 pm, respectively). PBE corrected for solids (PBEsol),[20] Wu-Cohen (WC), and its corrected description (WCsol)[21] have a MAE below 4 pm (3.7, 3.5, and 3.1 pm, respectively). The fully optimization of the structures has been performed using GGA-PBEsol because of its small error in predicting the relaxed structure and because the bandgaps are later calculated using a functional that is based on PBEsol.

The heats of formation of the candidate materials are calculated with respect to the cubic pure phases. For example, the heat of formation of the tetragonal $CsPbCl_2I$, $\Delta E_{CsPbCl_2I_{(t)}}$, is given by

$$\Delta E_{CsPbCl_2I_{(t)}} = E_{CsPbCl_2I_{(t)}} - \frac{2E_{CsPbCl_{3(c)}} + E_{CsPbI_{3(c)}}}{3}, \quad (1)$$

where E_{CsPbCl_2I} is the DFT total energy of the phase indicated in parentheses ((c): cubic and (t): tetragonal). When $\Delta E > 0$ eV/fu, the cubic pure systems are more stable than the candidate structure, while a negative ΔE indicates that the perovskite under investigation is favorable compared with the pure cubic phases. A more realistic evaluation of stability is obtained by calculating the heat of formation with respect to the most stable pure phases. In fact, the stability is, in this case, calculated with respect to a broader set of reference systems composed of all the possible phases that each compound can have, while only the cubic phases are included in the pool of references for Eq. (1). $\Delta E_{CsPbCl_2I_{(t)}}$ is now obtained using

$$\Delta E_{CsPbCl_2I_{(t)}} = E_{CsPbCl_2I_{(t)}} - \frac{2E_{CsPbCl_{3(o_1)}} + E_{CsPbI_{3(o_2)}}}{3}, \quad (2)$$

where (o_1) and (o_2) indicate the orthorhombic$_1$ and orthorhombic$_2$ phases, which are the most stable phases for $CsPbCl_3$ and $CsPbI_3$, respectively.

It is well-known that the Kohn-Sham states of standard DFT seriously underestimate the bandgaps. Possible solutions to this problem are the use of hybrid functionals or of many-body methods, that with an increase of the computational cost, give a better estimation of the optical properties of the materials. Alternatively, we here use the GLLB-SC potential by Gritsenko, van Leeuwen, van Lenthe, and Baerends (GLLB),[22] adapted by Kuisma *et al.*[23] to include the PBEsol correlation for solids (-SC) that has been shown to give reasonable bandgaps at a minimal cost.[14,24–26] This exchange-correlation functional includes explicitly the calculation of the derivative discontinuity (Δ_{xc}) that is added to the Kohn-Sham bandgap (E_{gap}^{KS}) to obtain the quasi-particle gap (E_{gap}^{QP}). GLLB-SC shows an agreement within 0.1 eV with respect to G_0W_0 for this class of systems.[45] It has been recently shown that the spin-orbit correction plays an important role in the estimation on

TABLE I. Comparison between the calculated (E_{gap}^{opt}) and experimental gaps (E_{gap}^{exp}), in eV, for a set of compounds. The MAE is also indicated.

Compound	Phase	E_{gap}^{opt}	E_{gap}^{exp}
$CsPbI_3$	Cubic	1.62	1.73[30]
$MASnI_3$	Tetragonal	1.51	1.20[31]
$MAPbBr_3$	Cubic	1.96	2.33[32]
$MAPbI_3$	Cubic	1.36	1.57[30]
$FAPbI_3$	Cubic	1.47	1.48[30]
MAE		0.20	

the bandgaps in particular for the cases of the lead perovskites.[27,28] The spin-orbit correction (Δ_{soc}) has been calculated using the Quantum Espresso code[29] for the Cs perovskites and has been seen to be dependent only on the B-ion and has the effect of reducing the bandgaps of 0.25 ± 0.05 eV in the case of Sn systems and of 1.02 ± 0.06 eV for Pb perovskites.

We have performed Bethe-Salpeter equation (BSE) calculations[33,44] for all the cubic systems with Cs^+ in the A site to calculate the reduction in the optical gap with respect to the quasiparticle gap due to electron-hole interactions.[46] We have observed that the reduction in the optical gap is always in a range from 0.11 to 0.15 eV.[47] Consequently we shifted down all the calculated band gaps in the screening process by $\Delta_{e-h} = 0.13$ eV.

The optical bandgap is thus obtained by

$$E_{gap}^{opt} = E_{gap}^{KS} + \Delta_{xc} - \Delta_{soc} - \Delta_{e-h}, \quad (3)$$

where Δ_{xc} is different for each system, while Δ_{soc} and Δ_{e-h} are *ad hoc* corrections based on calculations for a set of systems.

Table I reports the comparison between the calculated and experimental gaps of a set of compounds where the crystal structure is well determined. The agreement between DFT and experiments is very good with a MAE of 0.2 eV. In addition, the GLLB-SC gaps are comparable with other DFT bandgaps mentioned elsewhere in the literature.[27,28]

We investigate now the trends in the heat of formation and the bandgap of the calculated materials.

Fig. 2 shows the heats of formation for the investigated systems. For the Cs systems, all the combinations of anions are stable with respect to the cubic pure phases (Eq. (1)): in most of the cases they have a higher stability for an orthorhombic phase followed by the tetragonal phase and eventually by the cubic one. The phase transition from orthorhombic to cubic through tetragonal is a well-known phenomenon and has been already deeply investigated.[34–37] The situation is different when the heats of formation are calculated with respect to the most stable pure phases (Eq. (2)) where no combinations, except $FASnBr_2I$, are found to be stable. Despite of this, in most of the cases, the instability is rather small (less than 0.1 eV/fu) and in some cases probably beyond the accuracy of the calculation. Thus these systems might be slightly stable or metastable and at finite temperatures the entropy of mixing increases the stability of the mixed phases. In fact, some of the Cs mixed systems like $CsBr_2Cl$, $CsSnBr_2I$, and $CsSnBrI_2$ have been synthesized[38] as well as some of the MA mixed compounds like $MAPbClI_2$, $MAPbCl_2I$, and $MAPbI_2Br$.[39] However, one should note that photo-degradation may be an issue and depending on application instability in water could also require the use of protecting layers.[40,41]

Figure 3 shows the bandgaps as a function of the geometrical average of the electronegativities (in the Mulliken's scale[42]) of the anions for all the investigated perovskites. For example, the average electronegativity, χ, of the ClBrI combination is given by $\chi = (\chi_{Cl}\chi_{Br}\chi_I)^{1/3}$, where $\chi_{Cl} = 8.30$ eV, $\chi_{Br} = 7.59$ eV, and $\chi_I = 6.76$ eV are the electronegativities of Cl, Br, and I, respectively. The bandgaps increase with an increase of the electronegativity of the anions. Previous work[14] showed the effect of the electronegativities of the A- and B-ion on the gap. Here, we show that it is possible to substitute one or more anions with other species to tune the gap. Lower symmetries usually show larger gaps: the orthorhombic$_2$ phase has the largest bandgap between all the considered phases,

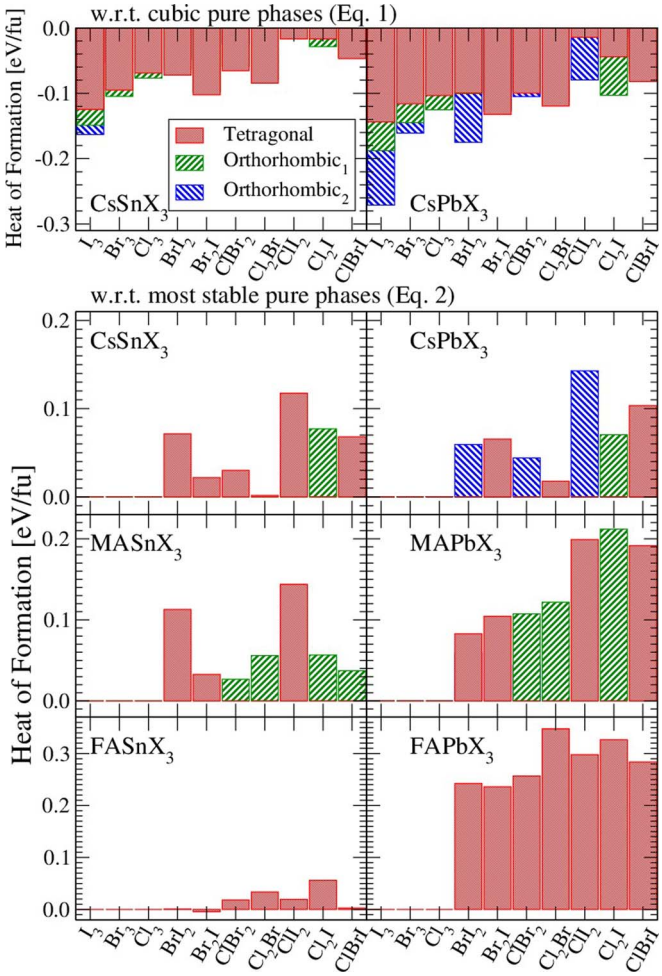

FIG. 2. Heats of formation with respect to the cubic pure phases using Eq. (1) (upper panel) and of the most stable phase with respect to the most stable pure phases using Eq. (2) (lower panels) for the investigated systems.

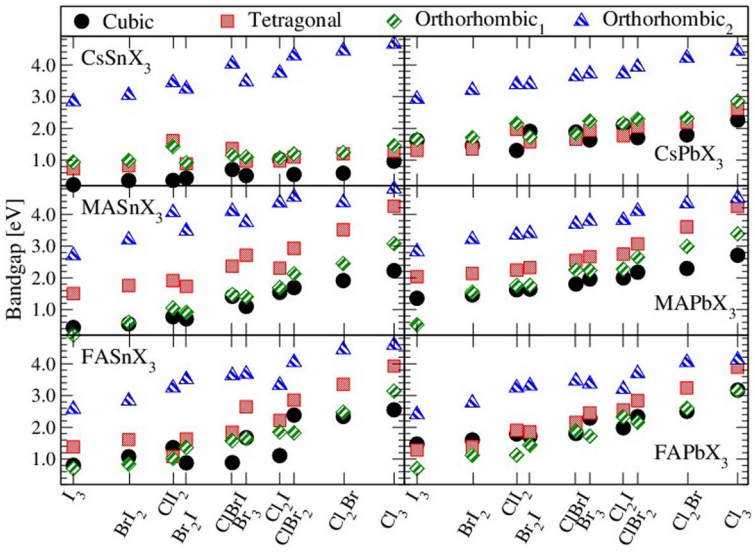

FIG. 3. Bandgaps as a function of the electronegativity of the anions for the investigated structures.

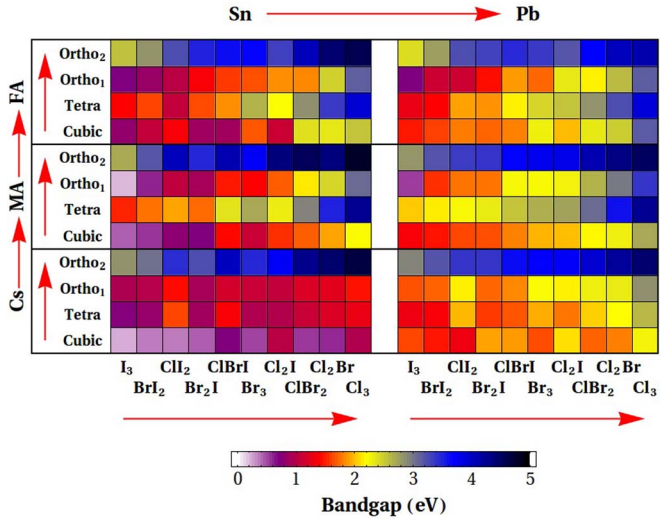

FIG. 4. Summary of the 240 calculated bandgaps. Each colored square corresponds to a different composition and phase. The A-ion and the phase can be identified by the labels on the left vertical axis, the B-ion and the anions composition (sorted for increasing electronegativity) from the labels on top and bottom of the horizontal axis, respectively. Red arrows follow the increase of the gaps with respect to changes in the cations, anions, and phases.

followed, in general by the orthorhombic$_1$ and tetragonal phases. The cubic phase shows the smallest gap but there are exceptions. In fact, the bandgap is not only determined by the electronegativities of the constituent elements, but also by the volume. It is well-known that there is a strong dependence of the bandgap upon the lattice parameter. In particular, Borriello *et al.*[1] found that the bandgap for the Sn cubic systems under stretching increases of approximately 2 eV/Å using PBE calculations. Using the GLLB-SC functional, we have observed that the bandgap increases linearly as 2.9, 3.4, and 3.6 eV/Å for the Sn systems with I_3, Br_3, and Cl_3 as anions, respectively, and of 2.2, 2.7, and 2.8 eV/Å for the Pb perovskites formed with I_3, Br_3, and Cl_3, respectively, i.e., the increase of the gap due to a change in the volume is also increasing with the electronegativity. Regarding instead the influence of the octahedron distortion upon the bandgap, we have studied the tilting of the XY_6 (X = Pb and Sn; Y = Cl, Br, and I) octahedra in the tetragonal phase with respect to the *c*-axis of the crystal without relaxing the structure. We found that the gap is reduced linearly with the tilting angle as ≈0.02 eV/°. In the real systems, the rotation of the octahedron is followed by changes in the lattice constants with the effect of increasing the bandgap.

Fig. 4 shows the bandgaps of all the calculated structures. The bandgaps span over a region from around 0.5 to around 5.0 eV. As shown also in Fig. 3, the bandgaps increase with the electronegativity of the anions (going from left to right in each half plot) and lowering the symmetry of the structure (from the bottom to the top of the plot for each A-ion). It is well-known that the bandgaps are influenced by the electronegativities of the cations.[14,43] In particular, the Sn systems have a smaller bandgap compared with the Pb perovskites. In the case of organometal perovskites, the A-ion changes the bandgap more because of the modification of the lattice constant than because of a change in the electronegativity. FA is larger than MA that is larger than Cs, and this results in a increase of the bandgap going from FA to Cs through MA. The trends described here are summarized with red arrows in the figure.

In this work, we have addressed the problem of calculating the bandgaps of all possible perovskites composed by Cs, MA, or FA as A-ions, Sn or Pb as B-ions, and Cl, Br, I, and their combinations as anions in their most common crystal symmetries (cubic, tetragonal, and orthorhombic), and we have investigated trends in their stability and bandgap.

The studied perovskites are usually stable in a tetragonal or orthorhombic phase and are expected to go through a phase transition towards the cubic symmetry at higher temperature. The bandgaps are strongly dependent on the electronegativities and on the lattice constants. In particular, the bandgap increases with an increase of the electronegativities of the B-ion and anions and with an

expansion of the lattices. The replacement of Cs with MA or FA has the effect of increasing the volume of the perovskite and so thus to increase the bandgap. The change in the gap due to a tilting of the octahedron has also been investigated. These trends indicate how to change the chemical composition to tune the bandgaps to a desired region.

The authors acknowledge support from the Catalysis for Sustainable Energy (CASE) initiative funded by the Danish Ministry of Science, Technology and Innovation and from the Center on Nanostructuring for the Efficient Energy Conversion (CNEEC) at Stanford University, an Energy Frontier Research Center founded by the US Department of Energy, Office of Science, Office of Basic Energy Sciences under Award No. DE-SC0001060. J.M.G.-L. also acknowledges support from the Spanish Ministry of Economy and Competitiveness under Projects FIS2010-21282-C02-01 and FIS2012-30996.

[1] I. Borriello, G. Cantele, and D. Ninno, Phys. Rev. B **77**, 235214 (2008).
[2] F. Chiarella, A. Zappettini, F. Licci, I. Borriello, G. Cantele, D. Ninno, A. Cassinese, and R. Vaglio, Phys. Rev. B **77**, 045129 (2008).
[3] Q. Chen, H. Zhou, Z. Hong, S. Luo, H.-S. Duan, H.-H. Wang, Y. Liu, G. Li, and Y. Yang, J. Am. Chem. Soc. **136**, 622 (2014).
[4] J. A. Christians, R. C. M. Fung, and P. V. Kamat, J. Am. Chem. Soc. **136**, 758 (2014).
[5] E. Edri, S. Kirmayer, D. Cahen, and G. Hodes, J. Phys. Chem. Lett. **4**, 897 (2013).
[6] E. Edri, S. Kirmayer, M. Kulbak, G. Hodes, and D. Cahen, J. Phys. Chem. Lett. **5**, 429 (2014).
[7] N. J. Jeon, J. Lee, J. H. Noh, M. K. Nazeeruddin, M. Grätzel, and S. I. Seok, J. Am. Chem. Soc. **135**, 19087 (2013).
[8] A. Kojima, K. Teshima, Y. Shirai, and T. Miyasaka, J. Am. Chem. Soc. **131**, 6050 (2009).
[9] G. Ceder, Y.-M. Chiang, D. R. Sadoway, M. K. Aydinol, Y.-I. Jang, and B. Huang, Nature (London) **392**, 694 (1998).
[10] W. Setyawan, R. M. Gaume, S. Lam, R. S. Feigelson, and S. Curtarolo, ACS Combinat. Sci. **13**, 382 (2011).
[11] J. Hachmann, R. Olivares-Amaya, S. Atahan-Evrenk, C. Amador-Bedolla, R. S. Sanchez-Carrera, A. Gold-Parker, L. Vogt, A. M. Brockway, and A. Aspuru-Guzik, J. Phys. Chem. Lett. **2**, 2241 (2011).
[12] N. M. O'Boyle, C. M. Campbell, and G. R. Hutchison, J. Phys. Chem. C **115**, 16200 (2011).
[13] I. Y. Kanal, S. G. Owens, J. S. Bechtel, and G. R. Hutchison, J. Phys. Chem. Lett. **4**, 1613 (2013).
[14] I. E. Castelli, T. Olsen, S. Datta, D. D. Landis, S. Dahl, K. S. Thygesen, and K. W. Jacobsen, Energy Environ. Sci. **5**, 5814 (2012).
[15] I. E. Castelli, D. D. Landis, K. S. Thygesen, S. Dahl, I. Chorkendorff, T. F. Jaramillo, and K. W. Jacobsen, Energy Environ. Sci. **5**, 9034 (2012).
[16] J. J. Mortensen, L. B. Hansen, and K. W. Jacobsen, Phys. Rev. B **71**, 035109 (2005).
[17] J. Enkovaara, C. Rostgaard, J. J. Mortensen, J. Chen, M. Dulak, L. Ferrighi, J. Gavnholt, C. Glinsvad, V. Haikola, H. A. Hansen *et al.*, J. Phys. Condens. Matter **22**, 253202 (2010).
[18] W. Kohn and L. J. Sham, Phys. Rev. **140**, A1133 (1965).
[19] J. P. Perdew, K. Burke, and M. Ernzerhof, Phys. Rev. Lett. **77**, 3865 (1996).
[20] J. P. Perdew, A. Ruzsinszky, G. I. Csonka, O. A. Vydrov, G. E. Scuseria, L. A. Constantin, X. Zhou, and K. Burke, Phys. Rev. Lett. **100**, 136406 (2008).
[21] Z. Wu and R. E. Cohen, Phys. Rev. B **73**, 235116 (2006).
[22] O. Gritsenko, R. van Leeuwen, E. van Lenthe, and E. J. Baerends, Phys. Rev. A **51**, 1944 (1995).
[23] M. Kuisma, J. Ojanen, J. Enkovaara, and T. T. Rantala, Phys. Rev. B **82**, 115106 (2010).
[24] F. Hüser, T. Olsen, and K. S. Thygesen, Phys. Rev. B **87**, 235132 (2013).
[25] I. E. Castelli, J. M. Garca-Lastra, F. Hüser, K. S. Thygesen, and K. W. Jacobsen, New J. Phys. **15**, 105026 (2013).
[26] I. E. Castelli, F. Hüser, M. Pandey, H. Li, K. S. Thygesen, B. Seger, A. Jain, K. Persson, G. Ceder, and K. W. Jacobsen, "New Light-Harvesting Materials Using Accurate and Efficient Bandgap Calculations," Adv. Energy Mater. (in press).
[27] P. Umari, E. Mosconi, and F. De Angelis, Sci. Rep. **4**, 4467 (2014).
[28] A. Amat, E. Mosconi, E. Ronca, C. Quarti, P. Umari, M. K. Nazeeruddin, M. Grätzel, and F. De Angelis, Nano Lett. **14**, 3608 (2014).
[29] P. Giannozzi, S. Baroni, N. Bonini, M. Calandra, R. Car, C. Cavazzoni, D. Ceresoli, G. L. Chiarotti, M. Cococcioni, I. Dabo *et al.*, J. Phys.: Condens. Matter **21**, 395502 (2009).
[30] G. E. Eperon, S. D. Stranks, C. Menelaou, M. B. Johnston, L. M. Herz, and H. J. Snaith, Energy Environ. Sci. **7**, 982 (2014).
[31] C. C. Stoumpos, C. D. Malliakas, and M. G. Kanatzidis, Inorg. Chem. **52**, 9019 (2013).
[32] G. Papavassiliou and I. Koutselas, Synthetic Metals **71**, 1713 (1995).
[33] E. E. Salpeter and H. A. Bethe, Phys. Rev. **84**, 1232 (1951).
[34] Y. Takahashi, R. Obara, Z.-Z. Lin, Y. Takahashi, T. Naito, T. Inabe, S. Ishibashi, and K. Terakura, Dalton Trans. **40**, 5563 (2011).
[35] Y. Kawamura, H. Mashiyama, and K. Hasebe, J. Phys. Soc. Jpn. **71**, 1694 (2002).
[36] K. Yamada, Y. Kuranaga, K. Ueda, S. Goto, T. Okuda, and Y. Furukawa, Bull. Chem. Soc. Jpn. **71**, 127 (1998).
[37] T. Sakudo, H. Unoki, Y. Fujii, J. Kobayashi, and M. Yamada, Phys. Lett. A **28**, 542 (1969).
[38] D. E. Scaife, P. F. Weller, and W. G. Fisher, J. Solid State Chem. **9**, 308 (1974).
[39] S. P. Singh and P. Nagarjuna, Dalton Trans. **43**, 5247 (2014).
[40] B. Cai, Y. Xing, Z. Yang, W.-H. Zhang, and J. Qiu, Energy Environ. Sci. **6**, 1480 (2013).

[41] G. Niu, W. Li, F. Meng, L. Wang, H. Dong, and Y. Qiu, J. Mater. Chem. A **2**, 705 (2014).
[42] R. S. Mulliken, J. Chem. Phys. **2**, 782 (1934).
[43] R. Aguiar, D. Logvinovich, A. Weidenkaff, A. Rachel, A. Reller, and S. G. Ebbinghaus, Dyes Pigments **76**, 70 (2008).
[44] A. Marini, C. Hogan, M. Grüning, and D. Varsano, Comput. Phys. Commun. **180**, 1392 (2009).
[45] We have calculated the GLLB-SC and G_0W_0 gaps for the MA pure systems in the cubic phase before the geometry optimization. The GLLB-SC and G_0W_0 calculated gaps are 2.27 and 2.30 eV for $MASnCl_3$, 1.25 and 1.29 eV for $MASnBr_3$, 0.70 and 0.89 eV for $MASnI_3$, 3.52 and 3.59 eV for $MAPbCl_3$, 2.88 and 2.83 eV for $MAPbBr_3$, and 2.29 and 2.27 eV for $MAPbI_3$.
[46] BSE calculations were performed on top of G_0W_0 results. Both BSE and G_0W_0 calculations were performed by means of the Yambo code[44] using as input electronic wavefunctions and energies from conventional DFT at PBE level results from the Quantum Espresso code. G_0W_0 calculations were performed including bands 50 eV above the Fermi level, in a 8 $\times$ 8 $\times$ 8 Monkhorst-Pack k-point grid[45] and using the Plasmon-Pole approximation.[46] Local field effects were taken into account. BSE calculations only included the closest 4 valence bands and 5 conduction bands to the Fermi level.
[47] Δ_{e-h} is equal to 0.14, 0.11, and 0.15 eV for $CsSnI_3$, $CsSnBr_3$, and $CsSnCl_3$, respectively, and to 0.12, 0.14, and 0.15 eV for $CsPbI_3$, $CsPbBr_3$, and $CsPbCl_3$, respectively.